Crossover behavior in interface depinning

Y. J. Chen

LASSP, Physics Department, Cornell University, Ithaca, New York 14853-2501, USA

Stefano Zapperi

Center for Complexity and Biosystems, Department of Physics, University of Milano, via Celoria 26, 20133 Milano, Italy;
CNR–Consiglio Nazionale delle Ricerche, IENI, Via R. Cozzi 53, 20125, Milano, Italy;
ISI Foundation, Via Alassio 11/c 10126 Torino, Italy;
and Department of Applied Physics, Aalto University, P.O. Box 14100, FIN-00076, Aalto, Finland

James P. Sethna

LASSP, Physics Department, Cornell University, Ithaca, New York 14853-2501, USA

We study the crossover scaling behavior of the height-height correlation function in interface depinning in random media. We analyze experimental data from a fracture experiment and simulate an elastic line model with nonlinear couplings and disorder. Both exhibit a crossover between two different universality classes. For the experiment, we fit a functional form to the universal crossover scaling function. For the model, we vary the system size and the strength of the nonlinear term and describe the crossover between the two universality classes with a multiparameter scaling function. Our method provides a general strategy to extract scaling properties in depinning systems exhibiting crossover phenomena.

I. INTRODUCTION

Driven interfaces in random media display intriguing scaling laws that are common to a wide variety of phenomena, including fluid imbibition, crack front roughening, dislocation hardening, superconducting flux lines, the equilibrium motion of piles of rice down an incline, and domain wall motion in magnets [1,2]. The scaling laws are commonly associated with an underlying depinning critical point that has been elucidated by simple models for interface dynamics. These models have been extensively studied using continuum simulations [3–6], cellular automata [3,7–11], and field-theoretic ϵ expansions [3,12–17], providing a sophisticated picture of the nonequilibrium phase transition and of the different universality classes.

The interface morphology is usually characterized by the roughness exponent ζ, resulting from a coarse graining operation of the interface height function $h(x)$. Namely, when we change all length scales by a factor b, or $x \to bx$, then statistically $h \to b^\zeta h$ – hence

$$h(x) \sim b^{-\zeta} h(bx). \tag{1}$$

For many experiments and simulations, it is convenient to measure ζ by computing the height-height correlation of the interface

$$C(r) = \langle [h(x+r) - h(x)]^2 \rangle \sim r^{2\zeta}. \tag{2}$$

[In Sec. II [18] we shall study a system with *anomalous scaling*, where the power law exhibited by $C(r)$ differs from the universal rescaling exponent ζ. Rather than rescaling h in such systems, one studies the rescaling of the correlation function directly, $C(r) \sim b^{-2\zeta} C(br) \sim r^{2\zeta}$. These systems are multiaffine [18]: different moments of h will scale with different exponents]. Here ζ should be uniquely determined by which universality class the system belongs to. However, in practice, the observed ζ varies (see Table I) even for the same type of system, such as paper wetting. Measuring a

single exponent for these systems may prove inadequate due to the presence of *crossover behavior* between universality classes. This is a common source of confusion and controversy. If the crossover is gradual, an experiment or simulation may measure an effective exponent ζ_{eff} intermediate between existing theories and appear to demand a new theoretical explanation (i.e., universality class).

In Sec. II we analyze a straightforward experimental example of a crossover between two forms of roughness in two-dimensional fracture. There we introduce the universal crossover scaling functions and provide a brief renormalization-group rationale.

In the remainder of the paper, we examine a more complex theoretical model. Crossovers, long studied in ordinary critical phenomena, have now been studied for several interface models [22]; however, theoretical studies have proven challenging in different ways [26]. For thin film magnets, the experiments [27–29] observe a crossover between short-range and mean-field universality classes as long-range dipolar fields are introduced, which can be done by changing the thickness of the film. However, for models of that type, simulations are challenging, because of both the long-range fields and the striking zig-zag morphologies that emerge and compete with the avalanche behavior. Crossovers involving the transition between depinning and sliding dynamics incorporating periodically correlated disorder [30] have also been studied. It is not typical, however, to study and report the universal scaling functions for these crossovers, a challenge we now shall address.

We shall analyze a numerically tractable, but analytically tricky, crossover [26]: the transition between the linear, super-rough, quenched Edwards-Wilkinson model (qEW) and the nonlinear quenched KPZ model (qKPZ) [2,22]. In both experiment and theory, we focus on the crossover behavior of the height-height correlation function.

TABLE I. Roughness exponents in experiments. Table reproduced from Ref. [1]. Notice that there is a wide range of ζ reported, even for the same experimental system.

Experiment	ζ	Reference
Fluid flow	0.73	[19]
	0.81	[20]
	0.65–0.91	[21]
Paper wetting	0.63	[22]
	0.62–0.78	[23]
Bacteria growth	0.78	[24]
Burning fronts	0.71	[25]

II. CROSSOVER IN FRACTURE SURFACE CORRELATIONS

Just as the critical exponent ζ is universal (independent of microscopic details, within a class of physical system), so too is the crossover behavior between universality classes. As a simple example, Santucci *et al.* [18] have measured a relatively sharp crossover between two regimes for two-dimensional fracture (inset in Fig. 1). Because the fracture is done slowly, we can view the crack front as self-organizing to the depinning transition for the crack front. Well below a critical distance r^*, they observe a power law $C(r) \sim r^{2\zeta_-}$ with an exponent that
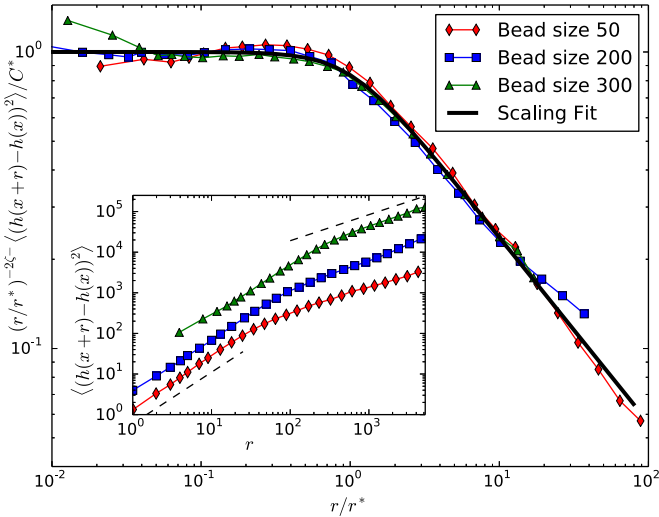

FIG. 1. (Color online) Crossover scaling in fracture roughness [18]. The inset shows experimental data for the height-height correlation function $C(r) = \langle [h(x+r) - h(x)]^2 \rangle$ of a 2D fracture front, generated by pulling apart two pieces of PMMA that have been sand-blasted and sintered together [18]. The three curves differ in the size of the sand-grain beads; the relation between the bead size and the toughness fluctuations in the PMMA were not measured. The dashed lines show two different power-law critical regimes, with $C(r) \sim r^{2\zeta_-}$ and $C(r) \sim r^{2\zeta_+}$, governing the short- and long-distance scaling behavior: the crossover between these regimes is evident. Our fit gives $\zeta_- = 0.63$ and $\zeta_+ = 0.32$, within the experimentalists' suggested range $\zeta_- = 0.6 \pm 0.05$ and $\zeta_+ = 0.35 \pm 0.05$. The main figure shows a scaling plot of $r^{-2\zeta_-} C(r)$ versus r, with the curves shifted vertically and horizontally to best collapse. The thick black curve is a one-parameter fit of the universal scaling function to the functional form in Eq. (4).

was interpreted as originating from coalescing cracks [31] or with Larkin scaling [32]. Well above r^* they observe a different power law $C(r) \sim r^{2\zeta_+}$ consistent with the depinning transition of a line [32–34]. The crossover between these two universal power-law regimes should be described by a *universal crossover function* [35], $\mathcal{C}_{\text{frac}}$:

$$C(r) \approx C^* r^{-2\zeta_-} \mathcal{C}_{\text{frac}}(r/r^*) \qquad (3)$$

independent of microscopic details. At small arguments $\mathcal{C}_{\text{frac}}(X)$ must go to a constant, and at large arguments $\mathcal{C}_{\text{frac}}(X) \sim X^{2(\zeta_- - \zeta_+)}$, so as to interpolate between the two power laws. When analyzing different systems governed by the same universal crossover, one may plot all the crossovers in a scaling plot, dividing the distances r on the ordinate by a system-dependent factor r^* for each curve, and dividing the magnitudes of the correlations on the abscissa by a system-dependent constant C^* (see Fig. 1). The resulting data curves then should align, giving the universal function $\mathcal{C}_{\text{frac}}(r/r^*)$.

To continue with this simple test case, we may fit the universal scaling function to an approximate functional form. (Indeed, we find it convenient to do a joint fit of the functional form, the exponents, and the constants r^* and C^*). To the extent that a guessed functional form reproduces the universal one, it is equivalent: advanced field-theoretic methods for calculating exact scaling functions are not needed to analyze future experiments. However, judicious choices of functional forms with the correct limiting behavior can greatly facilitate this process. The interpolation $1/(1 + X^{-2(\zeta_- - \zeta_+)})$ has the correct limits, but its rather gradual crossover does not explain the data. We may heuristically add a parameter n which at large values produces an abrupt crossover:

$$\mathcal{C}_{\text{frac}}(X) = [1 + (X^{2(\zeta_- - \zeta_+)})^{-n}]^{-1/n}. \qquad (4)$$

This yields an excellent fit to the data with $n \approx 4$ (see Fig. 1).

Why is the scaling form of Eq. (3) expected? Briefly, the renormalization group studies the behavior of systems under coarse graining: describing the properties of a system at length scales changed by a factor b. One gets universal power laws when the system becomes invariant under repeated coarse grainings: if $C(r) \rightarrow b^{2\zeta} C(r/b)$, under coarse graining by a factor b, then by coarse graining n times such that $r = b^n$ one has $C(r) \propto b^{2\zeta n} = r^{2\zeta}$. In the case of a crossover, a fixed point is unstable to some direction λ in system space. Then a small initial λ grows under rescaling by some factor $b^{1/\phi}$, so $C(r,\lambda) \rightarrow b^{2\zeta_-} C(r/b, \lambda b^{1/\phi})$. Now rescaling until $b^n = r$, we have

$$C(r,\lambda) \rightarrow b^{2n\zeta_-} C(r/b^n, \lambda b^{n/\phi}) = r^{2\zeta_-} C(1, \lambda r^{1/\phi})$$
$$= r^{2\zeta_-} \mathcal{C}_{\text{frac}}(\lambda^\phi r), \qquad (5)$$

where we choose $\mathcal{C}_{\text{frac}}(X) = C(1, X^{1/\phi})$. If the unstable direction flows to a new fixed point with a different ζ_+, that behavior will be reflected in the large-X dependence $C(X) \sim X^{2(\zeta_- - \zeta_+)}$ [36, Sec. 4.2]. Note that different physical systems will have different overall scales of height fluctuations, so we must have an overall scale C^* for each experiment. (If the experiments fall into a parameterized family, C^* will depend smoothly on the parameters, giving *analytic corrections to scaling* as discussed in Sec. IV). Note, though, that the

rescaling factor r^* for lengths, while it will still vary from one system to another, now depends on λ with a power-law singularity, as $r^* = 1/\lambda^{\phi}$; within the renormalization group, λ measures how far along the unstable direction the original system was poised. In particular, r^* becomes large as $\lambda \to 0$, as in that limit the unstable fixed point remains in control.

The three experiments depicted in Fig. 1 started with different bead sizes. If all other features of the experiment are held fixed, one may assume that the control parameter λ depends in some smooth way on the bead size. Had we several values of bead size, we could then extract values for the universal crossover exponent ϕ.

In the following sections, we shall perform a far more sophisticated version of this type of analysis. By exhaustively varying system size and nonlinearity in an interface growth model, we shall not only generate universal *two-variable* functional forms for the correlation crossover scaling function, but will be able to make predictions about both the dependence of the crossover length scale (corresponding to r^*) and the dependence of the correlation amplitude (corresponding to C^*) on the control parameters. A rich, nuanced understanding of the model behavior thus emerges.

III. LINE DEPINNING MODEL

The equations of an interface in a disordered environment may be written generally as follows. Let the one-dimensional interface, $h(x,t)$ be driven by a force $H(t)$ through a disordered environment with a local quenched random force $\eta(h(x),x)$:

$$\frac{\partial h}{\partial t} = \gamma \nabla^2 h + \lambda (\nabla h)^2 + \eta(h(x),x) - k \langle h \rangle_x + H(t). \quad (6)$$

Here γ is a surface tension, and λ is the coefficient of the KPZ term. The KPZ term controls lateral spreading of the interface, breaks the statistical tilt symmetry, and changes the universality class [1]. $H(t)$ is a slowly increasing external driving force. Our simulations are done with a lattice automaton; the lattice naively might be thought to break this statistical tilt symmetry, but simulations have long shown that the model faithfully describes both universality classes [37].

The term $-k \langle h \rangle_x$ is borrowed from simulations of magnets, where it represents the demagnetization force [38], approximating the effects of the long-range dipolar field cost of a net advance in the front. This restoring force "self-organizes" the depinning transition to the fixed point, allowing simulations to access many metastable states, without having to enforce an actual quasistatic field. It is known [39] that this restoring force does not produce loop corrections to the renormalization group equations and therefore does not change the universality class of the problem. We have confirmed numerically that its effects are small for our crossover and appear irrelevant. As the restoring force makes the simulation vastly more efficient, we include this restoring force, but we do not include k in our scaling analysis.

IV. ANALYSIS OF CROSSOVER SCALING

Using the automaton simulation employed in Ref. [40], we tune λ / γ from 0 to 5 and observe how the resulting behavior changes. Figure 2 shows how the front morphology qualitatively changes while we increase the nonlinear parameter λ. Notice that with increasing λ the fronts between events are flatter than at small λ.

According to Eq. (2), naively one would assume we could recover the exponent ζ by defining an effective exponent ζ_{eff} to be half the local-log slope of the height-height correlation functions (Fig. 3). From other numerical studies, for qEW, we expect $\zeta_{\text{EW}} \simeq 1.25$. (Cellular automata [8,41] models show $\zeta_{\text{EW}} = 1.25 \pm 0.01$; continuous string models [42] found $\zeta_{\text{EW}} \approx 1.26$.) For qKPZ, we expect $\zeta_{\text{KPZ}} = 0.63$ [11,43]. However, there are two things about Fig. 3 worth noting: (1) the slope measure of ζ drifts between 0.63 and 1.0 as we change λ, and (2) the measured value is never greater than one as is naively expected for the linear qEW model. The dropoff at $r \sim L/4$ is due to the periodic boundary conditions.

The second issue has a known resolution: for $\zeta > 1$, when the interface is "super-rough," the height cannot grow faster than linearly with distance, so the height-height correlation function cannot directly exhibit a power law larger than one [44]. This so-called anomalous scaling [45–47] implies that the
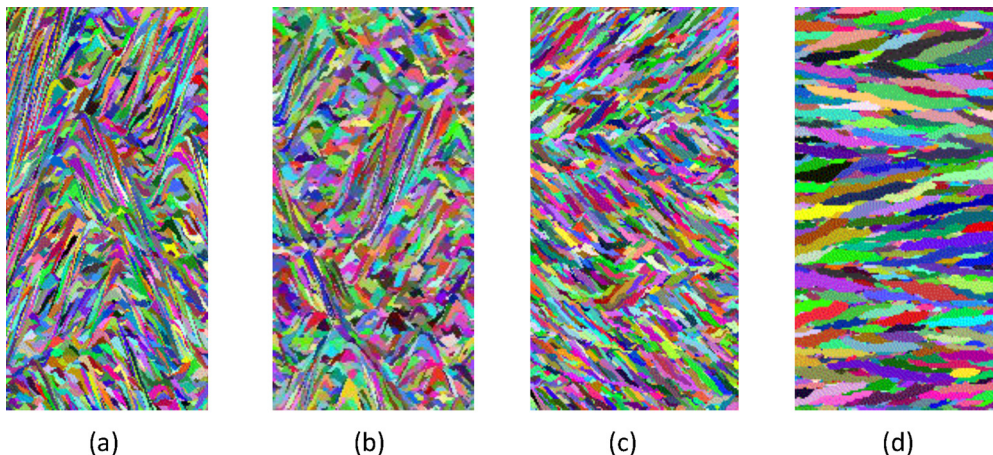

FIG. 2. (Color online) Crossover of qKPZ to qEW model. Fronts generated from 128×256 simulations with the nonlinear KPZ term coefficients set to (a) $\lambda = 0$, (b) $\lambda = 0.001$, (c) $\lambda = 0.1$, (d) $\lambda = 5$. The random colors (shades) represent the area between each pinned front. The morphology of the interfaces changes dramatically as λ increases.
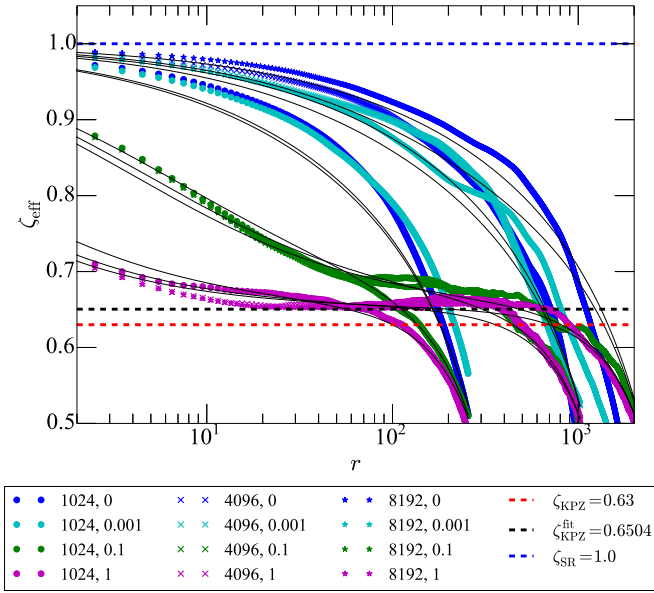
FIG. 3. (Color online) Local log slope. The measured local-log slope, $d \log C / d \log r$ of the height-height correlation function for varying λ and $k = 0.01$. The lower dashed red line is $\zeta_{KPZ} = 0.63$ as expected for the KPZ universality class. The upper dashed blue line is $\zeta_{SR} = 1.0$, the largest growth allowed for super-rough interfaces. The thin lines show the predictions of our fits (Sec. IV), and the dashed black line is the fit value of ζ_{KPZ}. The sharp cutoff in the curves at large r is due to the periodic boundary condition, which forces $\zeta_{eff} = 0$ at $r = L/2$; the larger L curves have later cutoffs. As expected, for small λ the curves are described by the EW behavior $\zeta_{SR} = 1$ at small r, while for large λ they are well described by ζ_{KPZ}. For intermediate values of $\lambda \sim 0.1$, we observe a clear transition from EW behavior at small r to KPZ behavior at intermediate r, before being cut off by the finite size effects.

exponent ζ is reflected not in the distance dependence of the correlation function, but rather in its *system-size dependence*. We thus consider the finite-size scaling form

$$C_{EW}(r|L) \sim L^{2\zeta_{EW}}(r/L)^2 \mathcal{C}_{EW}(r/L); \quad (7)$$

the roughness exponent ζ_{EW} may be estimated by the system-size dependence of the magnitude of C_{EW}. Note that the periodic boundary conditions implies that $C_{EW}(r|L) = C_{EW}(-r|L) = C_{EW}(L - r|L)$; near $r = L/2$ the correlation function reaches a peak (and ζ_{eff} vanishes, as in Fig. 3). Thus $X^2\mathcal{C}_{EW}(X) = (1 - X)^2\mathcal{C}_{EW}(1 - X)$. To control the sharpness of the peak in the correlation function at $X = 1/2$, in analogy to the crossover sharpness parameter n of Eq. (4), we introduce n_{EW} giving a transition between the two power laws:

$$X^2\mathcal{C}_{EW}(X) = \{(X^2)^{-n_{EW}} + [(1 - X)^2]^{-n_{EW}}\}^{-1/n_{EW}}. \quad (8)$$

For qKPZ [Fig. 2(c)], the correlation function in a system size L takes the finite-size scaling form

$$C_{KPZ}(r|L) = Ar^{2\zeta_{KPZ}}\mathcal{C}_{KPZ}(r/L), \quad (9)$$

where we introduce n_{KPZ} to form a periodic functional form

$$X^{2\zeta_{KPZ}}\mathcal{C}_{KPZ}(X) = \{(X^{2\zeta_{KPZ}})^{-n_{KPZ}}$$
$$+ [(1 - X)^{2\zeta_{KPZ}}]^{-n_{KPZ}}\}^{-1/n_{KPZ}}. \quad (10)$$

The drift in the exponent ζ, however, demands a study of the scaling near the unstable qEW fixed point and the functional form of the resulting crossover scaling function. The role of λ in generating the crossover from qEW to qKPZ has only been studied qualitatively [4,7,10,11], with no full description of the crossover scaling [26]. The crossover describes the RG flow from the qEW fixed point to the qKPZ as the relevant parameter λ is added. The scaling form for the height-height correlation function is thus that of a relevant variable λ added to the qEW scaling:

$$C(r|L,\lambda) = L^{2\zeta_{EW}}\mathcal{C}(r/L,\lambda^{\phi}r). \quad (11)$$

For $\lambda \gg 0$, $C(r|L,\lambda) \to C_{KPZ}(r|L)$; therefore,

$$\mathcal{C}(r/L,\lambda^{\phi}r)$$
$$\to A(\lambda)r^{2\zeta_{KPZ}}\mathcal{C}_{KPZ}(r/L)/L^{2\zeta_{EW}}$$
$$= A(\lambda)(r/L)^{2\zeta_{KPZ}}L^{-2(\zeta_{EW}-\zeta_{KPZ})}\mathcal{C}_{KPZ}(r/L)$$
$$= A_{analytic}(\lambda)(r/L)^{2\zeta_{KPZ}}(\lambda^{\phi}L)^{-2(\zeta_{EW}-\zeta_{KPZ})}\mathcal{C}_{KPZ}(r/L). \quad (12)$$
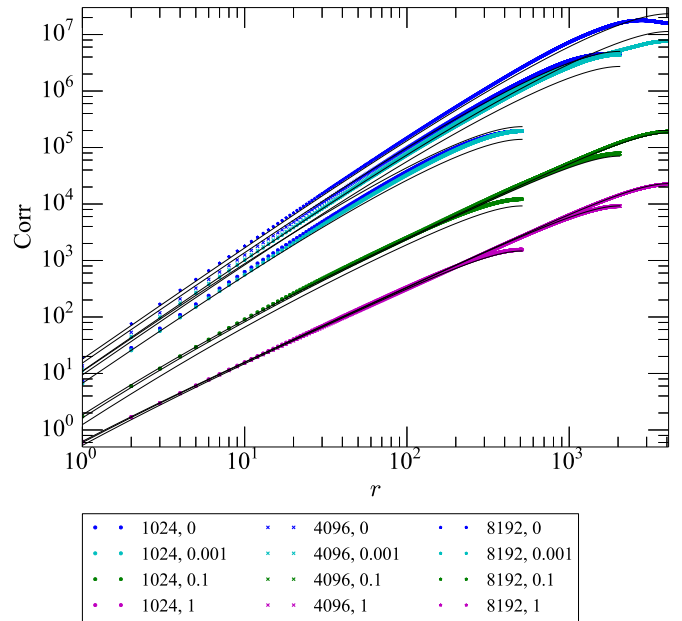

FIG. 4. (Color online) Height-height correlation function. The numerics generated with an automata code (symbols) are well described by Eq. (16) (black curves) with fit parameters $\phi = 1.0 \pm 0.4$, $\zeta_{KPZ} = 0.65 \pm 0.04$, $\zeta_{EW} = 1.1 \pm 0.15$, $n_{Cross} = 1.0 \pm 0.7$, $B = 2.5 \pm 6.0$, $n_{EW} = 0.27 \pm 0.03$, $n_{KPZ} = 1.1 \pm 0.6$, $A_0 = 2.7 \pm 7$, $A_1 = 770 \pm 900$, and $A_{\infty} = 0.3 \pm 1$. (A fit constrained to the expected values of ζ_{EW} and ζ_{KPZ} give slightly worse, but acceptable fits, with the other parameter estimates within the quoted ranges). The legends denote L and λ for each simulated correlation function; all runs had $k = 0.01$. The errors quoted are a rough measure of the systematic error [48], as described in the text, and are representative of the differences we find using different weightings and functional forms. (They are much larger than the statistical errors). The amplitude dependence is captured by the scaling form. Three of the 12 parameters (ζ_{EW}, ζ_{KPZ}, and ϕ) are universal critical exponents, three (A_0, A_1, and A_{∞}) describe the nonuniversal dependence of an overall height scale on parameters, two describe finite-size effects, and only two (n_{Cross} and B) are needed to describe the universal crossover function to the accuracy shown.
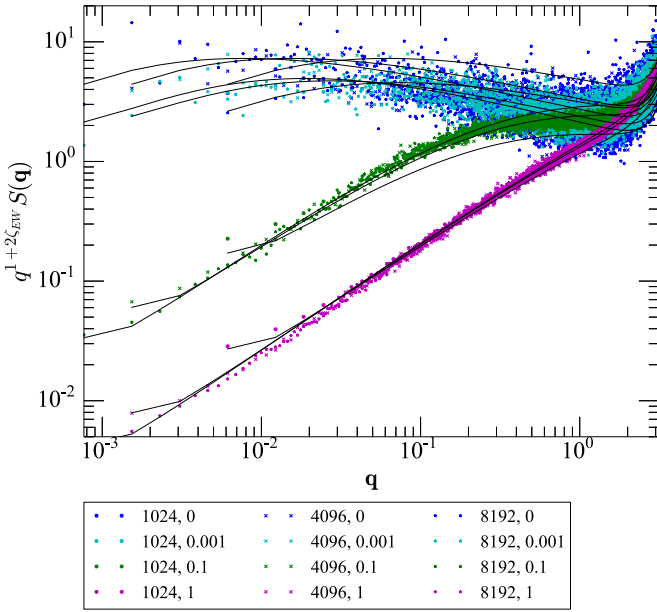
FIG. 5. (Color online) Rescaled spectral function $S(q|L,\lambda)$ for the height fluctuations. Rescaling by the naive RG power $q^{1+2\zeta_{EW}}$ does collapse the data for vanishing λ (up to a significant noise): the anomalous scaling for the super-rough interface in real space is not manifested in Fourier space. The theory curves are given by the Fourier transform of the same best fit shown in previous figures.

Here $A(\lambda)$ is in general a nonuniversal prefactor for the KPZ correlation function. As with C^* in Sec. II, A is expected to vary [49] with the parameters of the problem.
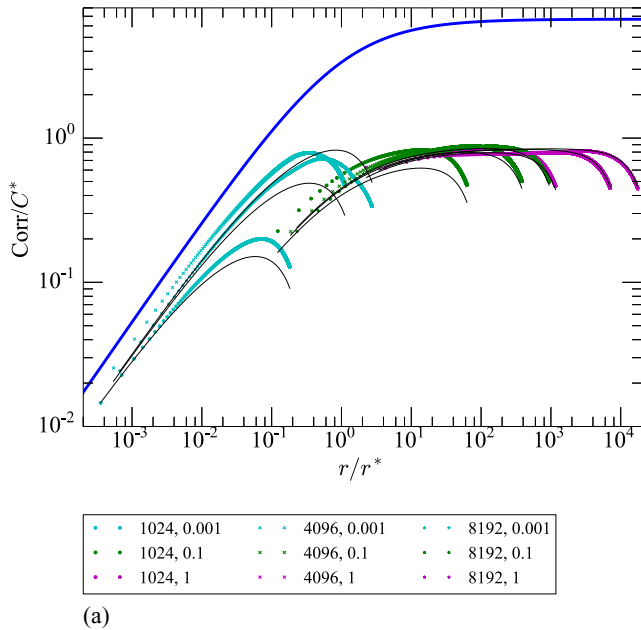
Here it has a typical smooth variation $A_{\text{analytic}}(\lambda)$, times a singular piece $A_{\text{singular}}(\lambda)$ due to the EW fixed point: $A(\lambda) = A_{\text{analytic}}(\lambda)A_{\text{singular}}(\lambda)$. We derive the power-law divergence of the amplitude

$$A_{\text{singular}}(\lambda) = \lambda^{-2(\zeta_{EW} - \zeta_{KPZ})\phi} \tag{13}$$

by noting that $\mathcal{C}(r/L, \lambda^\phi r)$ must be a scaling function with only invariant combinations of r, L, λ.

We must also have $\mathcal{C}(r/L, 0) \sim (r/L)^2 C_{EW}(r|L)$. Using these limits, Eq. (14), and the fact that $A(\lambda)$ gets large as $\lambda \to 0$ and small as $\lambda \to \infty$, we can construct a function that crosses over between these two limits:

$$
\begin{aligned}
C(r|L,\lambda) &= A_{\text{analytic}}\{[A_{\text{singular}}(\lambda)BC_{KPZ}(r/L)]^{-n_{\text{Cross}}} \\
&\quad + C_{EW}(r/L)^{-n_{\text{Cross}}}\}^{-1/n_{\text{Cross}}} \\
&= L^{2\zeta_{KPZ}}\mathcal{C}(X,Y), \tag{14}
\end{aligned}
$$

where $X = r/L$ and $Y = \lambda^\phi r$, and C_{KPZ} and C_{EW} are defined in Eqs. (7)–(10). We expand the analytic function $A_{\text{analytic}} = (A_0 - A_\infty)/(1 + A_1\lambda) + A_\infty$ in a form analytic at zero and saturating at large λ at A_∞[50], and we include a relative scale factor B. Finally, we vary the sharpness of the crossover with n_{Cross}, just as we did in the experimental study of fracture [Eq. (4)].

The theoretical curves in were fit to the data in Figs. 3, 4, and 5, deleting the noisy half near $r = L/2$ in the first, and using weights $\sigma^2 \sim \sqrt{r/L}$ designed to equalize the emphasis on each decade. The errors quoted are a rough estimate of the systematic error [48] given by quadratically exploring fits with roughly twice the ξ^2 of the best fit.

(a)
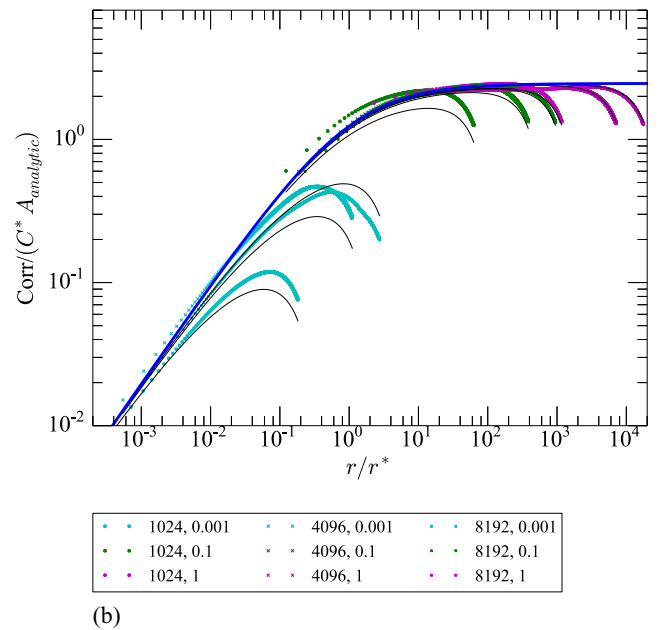
(b)

FIG. 6. (Color online) Scaling collapse of the height-height correlation function. The correlation-function data of Fig. 4 are collapsed to illustrate the crossover between EW and KPZ-dominated lengths ($r < r^*$ and $r > r^*$, respectively; see also Refs. [28,29]). Here $r^* = L[B(L\lambda^\phi)^{2(\zeta_{EW} - \zeta_{KPZ})}]^{-1/(2-2\zeta_{KPZ})}$ is the distance where the EW and KPZ components of the correlation function are equal in magnitude, and $C^* = \lambda^{-2\phi(\zeta_{EW}-\zeta_{KPZ})}r^{2\zeta_{KPZ}}$ factors out the dependence expected in the KPZ regime (hence yielding flat behavior for $r \gg r^*$). (b) Effects of analytic corrections to scaling are also factored out; all of the curves lie on a universal curve apart from the effects of the finite system sizes (causing each curve to drop on the right). (a) The analytic correction to scaling has a significant impact on the scaling collapse: ignoring it in the analysis would produce significant errors in critical exponents and scaling functions. The thick blue curve shows the scaling function prediction for the crossover [which, if $x = r/r^*$, can be shown to be $C/C^* = Bx^2(x^{2n_{\text{Cross}}} + x^{2n_{\text{Cross}}\zeta_{KPZ}})^{-1/n_{\text{Cross}}}$].

Note that this gives us a universal function of three variables (r, L, and λ). Note that it predicts a singularity at small λ in the form of a divergent amplitude $A_{\text{sing}} \sim \lambda^{-2(\zeta_{\text{EW}} - \zeta_{\text{KPZ}})\phi}$ in the qKPZ correlation function [Eq. (9)] as $\lambda \to 0$. This universal singularity in the amplitude (corresponding to a prediction of C^* in Sec. II) explains the amplitude dependence seen in Fig. 4. There is an analogous universal amplitude dependence seen for the Heisenberg $\to$ Ising crossover at small Ising anisotropy [36, Sec. 4.1].

We can use the scaling form of the correlation function $C(r|L,\lambda)$ to derive other, less complex crossover scaling functions traditionally studied in interface depinning problems [30,42]. The spectral scaling function is equal to the Fourier transform of our correlation function (with subtleties at $q = 0$):

$$S(q|L,\lambda) = |\tilde{h}(q)|^2 = \int_r C(r|L,\lambda) \exp(iqr)\, dr$$
$$\sim q^{-1-2\zeta_{\text{EW}}} \mathcal{S}(\lambda^{-\phi}q, qL). \quad (15)$$

Here the universal spectral crossover scaling function $\mathcal{S}(\tilde{X}, \tilde{Y})$ can be written in terms of our universal correlation crossover scaling function [$\mathcal{C}(X,Y)$ from Eq. (11)] as

$$\mathcal{S}(\tilde{X}, \tilde{Y}) = \int dz \exp(iz)\tilde{Y}^{2\zeta_{\text{EW}}} \mathcal{C}(z/\tilde{Y}, z/\tilde{X}) \quad (16)$$

depicted in Fig. 5. Here it is known that $\mathcal{S}$ does not have anomalous scaling; the power laws ζ_{EW} and ζ_{KPZ} can be read off from the slopes at large and small $\tilde{Y}$. More ordinary, single-variable scaling functions can be derived from our two-variable scaling functions, such as that governing the average width of an interface [given by the zero Fourier component of $S(q)$ or an integral of $C(r)$]; such scaling functions [as for the fracture scaling function of Eq. (3)] allow traditional scaling collapses (as in Fig. 1). However, one should note that our analyzed simulations extend to $\lambda \sim 1$, where analytic corrections to scaling, as vividly illustrated in Fig. 6(a), would likely invisibly distort the resulting scaling collapses. It is an advantage of multivariable scaling fits that they both allow the incorporation of such analytic corrections (extending the range of applicability) and force their incorporation (exposing weaknesses of the naive theory).

V. CONCLUSIONS

In this paper, we have analyzed the scaling properties for an experimental 2D fracture front and a model of an interface moving in random media, focusing on the crossover scaling of the roughness. The experimental system is successfully modeled using a one-variable universal scaling function with one free parameter, controlling the sharpness of the transition. The theoretical model, the crossover from the qEW to the qKPZ universality class with the addition of a nonlinear term, allows us to estimate the complete universal scaling function for the height-height correlation function including both finite-

size effects and the nonlinear effects of the tuning parameter λ, while satisfying known limits given by the renormalization group.

We emphasize the importance of our sophisticated use of the scaling forms and corrections predicted from renormalization group. Figure 1 illustrates that not only the power laws, but the entire functional form of the crossover, is a universal property that should be reported. Equation (4) is an effective one-parameter way of embodying the sharpness of the crossover, which we use also in the theoretical analysis of Sec. IV for both the crossover and the effects of periodic boundary conditions. Figures 3, 4, and 5 show how different experimental characterizations of the roughness of an interface can be simultaneously fit with a single functional form. Figure 6(a) vividly indicates the importance of analytic corrections to scaling in extending the validity of the theoretical analysis to smaller systems and farther outside the critical region. Only systems with $\lambda < 10^{-3}$ will follow the scaling behavior without incorporating the analytic corrections, while the entire crossover is faithfully represented in Fig. 6(b) by including them in the fit.

By developing functional forms for the correlation functions [40], we gain the flexibility of incorporating analytic corrections, multiple scaling variables, and a systematic error analysis while allowing the quantitative reporting of the universal scaling functions. One should note that the parameter estimation errors quoted here are large compared to more traditional scaling analyses. In part this is due to our estimation of the relevant systematic errors [48]; statistical errors would be perhaps an order of magnitude smaller. In part, however, this is due to our incorporation of known but usually ignored confounding factors; analytic corrections to scaling and crossover effects will invisibly distort the results of more direct measurements, and the drift in exponents quoted in the literature in critical phenomena often exceeds the error estimates.

It is challenging but satisfying to develop these functional forms. Measuring and fitting them is far more physically intuitive and less technically demanding than direct field-theoretic calculations [42] (although theoretical calculations often form important inspiration for choosing functional forms [40]). Successful functions are parsimonious in the number of adjustable parameters, and developing them often forces one to develop a far more complete understanding of the physics of the system under consideration.

[1] A. L. Barabási and H. E. Stanley, *Fractal Concepts in Surface Growth* (Cambridge University Press, Cambridge, 1995).

[2] M. Kardar, Phys. Rep. **301**, 85 (1998).

[3] H. Leschhorn, T. Nattermann, S. Stepanow, and L. H. Tang, Ann. Physik **6**, 1 (1997).

[4] A. Rosso and W. Krauth, Phys. Rev. Lett. **87**, 187002 (2001).

[5] A. Rosso and W. Krauth, Phys. Rev. E **65**, 025101 (2002).

[6] A. Rosso, A. K. Hartmann, and W. Krauth, Phys. Rev. E **67**, 021602 (2003).

[7] L.-H. Tang and H. Leschhorn, Phys. Rev. A **45**, R8309(R) (1992).

[8] H. Leschhorn, Physica A **195**, 324 (1993).

[9] H. Leschhorn, J. Phys. A **25**, L555 (1992).

[10] H. Leschhorn and L.-H. Tang, Phys. Rev. E **49**, 1238 (1994).

[11] H. Leschhorn, Phys. Rev. E **54**, 1313 (1996).

[12] O. Narayan and D. S. Fisher, Phys. Rev. B **46**, 11520 (1992).

[13] O. Narayan and D. S. Fisher, Phys. Rev. B **48**, 7030 (1993).

[14] O. Narayan and A. A. Middleton, Phys. Rev. B **49**, 244 (1994).

[15] P. Chauve, T. Giamarchi, and P. Le Doussal, Phys. Rev. B **62**, 6241 (2000).

[16] P. Chauve, P. Le Doussal, and K. J. Wiese, Phys. Rev. Lett. **86**, 1785 (2001).

[17] P. Le Doussal, K. J. Wiese, and P. Chauve, Phys. Rev. B **66**, 174201 (2002).

[18] S. Santucci, M. Grob, A. Hansen, R. Toussaint, J. Schmittbuhl, and K. J. Måløy, Eur. Phys. Lett. **92**, 44001 (2010).

[19] M. A. Rubio, C. A. Edwards, A. Dougherty, and J. P. Gollub, Phys. Rev. Lett. **63**, 1685 (1989).

[20] V. K. Horvath, F. Family, and T. Vicsek, J. Phys. A **24**, L25 (1991).

[21] S. He, G. L. M. K. S. Kahanda, and P.-Z. Wong, Phys. Rev. Lett. **69**, 3731 (1992).

[22] S. V. Buldyrev, A.-L. Barabási, F. Caserta, S. Havlin, H. E. Stanley, and T. Vicsek, Phys. Rev. A **45**, R8313(R) (1992).

[23] F. Family, K. C. B. Chan, and J. G. Amar, in *Surface Disordering: Growth, Roughening and Phase Transitions* (Nova Science, New York, 1992), pp. 205–212.

[24] T. Vicsek, M. Cserzö, and V. K. Horváth, Physica A **167**, 315 (1990).

[25] J. Zhang, Y.-C. Zhang, P. Alstrom, and M. T. Levinsen, Physica A **189**, 383 (1992).

[26] P. Le Doussal and K. J. Wiese, Phys. Rev. E **67**, 016121 (2003).

[27] D.-H. Kim, S.-B. Choe, and S.-C. Shin, Phys. Rev. Lett. **90**, 087203 (2003).

[28] K.-S. Ryu, H. Akinaga, and S.-C. Shin, Nat. Phys. **3**, 547 (2007).

[29] J. P. Sethna, Nat. Phys. **3**, 518 (2007).

[30] S. Bustingorry, A. B. Kolton, and T. Giamarchi, Phys. Rev. B **82**, 094202 (2010).

[31] J. Schmittbuhl, A. Hansen, and G. G. Batrouni, Phys. Rev. Lett. **90**, 045505 (2003).

[32] L. Laurson, S. Santucci, and S. Zapperi, Phys. Rev. E **81**, 046116 (2010).

[33] J. Schmittbuhl, S. Roux, J.-P. Vilotte, and K. J. Måløy, Phys. Rev. Lett. **74**, 1787 (1995).

[34] A. Rosso and W. Krauth, Phys. Rev. B **65**, 012202 (2001).

[35] D. R. Nelson, Phys. Rev. B **11**, 3504 (1975).

[36] J. Cardy, *Scaling and Renormalization in Statistical Physics*, vol. 5 (Cambridge University Press, Cambridge, 1996).

[37] L. A. N. Amaral, A.-L. Barabási, H. A. Makse, and H. E. Stanley, Phys. Rev. E **52**, 4087 (1995).

[38] G. Durin and S. Zapperi, in *The Science of Hysteresis*, Vol. 2 (Academic Press, New York, 2006), pp. 181–267.

[39] O. Narayan, Phys. Rev. Lett. **77**, 3855 (1996).

[40] Y.-J. Chen, S. Papanikolaou, J. P. Sethna, S. Zapperi, and G. Durin, Phys. Rev. E **84**, 061103 (2011).

[41] M. Jost and K. Usadel, Physica A **255**, 15 (1998).

[42] A. Rosso, P. Le Doussal, and K. J. Wiese, Phys. Rev. B **75**, 220201 (2007).

[43] C. Lee and J. M. Kim, J. Korean Phys. Soc. **47**, 13 (2005).

[44] H. Leschhorn and L.-H. Tang, Phys. Rev. Lett. **70**, 2973 (1993).

[45] J. M. López, M. A. Rodriguez, and R. Cuerno, Phys. Rev. E **56**, 3993 (1997).

[46] J. M. López and J. Schmittbuhl, Phys. Rev. E **57**, 6405 (1998).

[47] J. J. Ramasco, J. M. López, and M. A. Rodriguez, Phys. Rev. Lett. **84**, 2199 (2000).

[48] S. L. Frederiksen, K. W. Jacobsen, K. S. Brown, and J. P. Sethna, Phys. Rev. Lett. **93**, 216401 (2004).

[49] There are other analytic corrections to scaling that will in general become important at long distances from the critical point. For example [36, Section 3.3], λ is presumably not the natural measure of the unstable direction in parameter space; in general that would be an analytic function $u_\lambda \propto \lambda + O(\lambda^2)$ of λ and other parameters.

[50] Indeed, simulations at $\lambda = 2$ and $\lambda = 5$ indicate a saturation of the amplitude of the KPZ power-law scaling. This suggests that $A_{\text{analytic}}(\lambda) \propto 1/A_{\text{singular}}(\lambda)$ at larger λ. In the range we consider, an asymptotically flat asymptote suffices to capture this variation; independent fits of the amplitude at each λ including the larger systems give comparable fits and other parameters within our ranges.